Failure analysis of laminated tubes under tension-torsion biaxial loading

†Jingmeng Weng [1], *Weidong Wen [1], Haitao Cui [1], Ying Xu [1], Yaoxia Huo [1]

[1] Jiangsu Province Key Laboratory of Aerospace Power System, Nanjing 210016, P.R. China
State Key Laboratory of Mechanics and Control of Mechanical Structures, Nanjing 210016, P.R. China
College of Energy & Power Engineering, Nanjing University of Aeronautics and Astronautics, Nanjing 210016, P.R. China

*Presenting author: wjm19890606@126.com
†Corresponding author: jm_weng@nuaa.edu.cn

Abstract

An experimental and numerical study of laminated tubes with $[45^\circ/70^\circ/-45^\circ/0^\circ{}_2]_s$ under different combinations of tension-torsion biaxial loading is presented. The effect of biaxiality ratio on biaxial strength is discussed. Moreover, a progressive damage model to simulate the failure behaviour of laminated tubes under different combinations of tension-torsion biaxial loading is presented. The main advantage of the model is that it can simulate the failure behavior of laminated tubes under combined tension-torsion biaxial loading by using the experimental results of unidirectional flat specimens. The maximum error between predicted strength and experimental results is within 9%. The experimental and numerical results show that the axial load carrying capacity of tubular specimen decreases rapidly as biaxiality ratio increases.

Keywords: Laminated tubular specimen, Biaxial loading, Biaxial strength prediction model

Introduction

Due to their superior strength-to-weight and modulus-to-weight ratios, fiber reinforced composite materials are widely used in military and commercial applications, such as airplanes and motor vehicles. The majority of these structural components in service are subjected to biaxial or triaxial state of stress.

If the goal of biaxial testing is to generate a failure envelope in σ_1-σ_2 stress space, cruciform specimen is the most appropriate choice. Under biaxial loading, the distribution and repartition of stress is not constant over the cruciform specimen. Therefore, strain field monitoring techniques are required, such as strain gages or strain rosettes [1], high-speed stereo digital image correlation [2], infrared thermography[3], air-coupled guided waves [3], and digital image correlation [4, 5], etc. Test monitoring and numerical simulation [1-11] have demonstrated that it’s almost impossible to eliminate the stress concentration in the milled zone and the outer fillet corner between two perpendicular arms.

Thin tubular specimens avoid problems associated with stress concentrations and free edges effects that are encountered with cruciform specimens, and a wide range of biaxial and triaxial stress space can be applied by subjecting tubular specimens to different combinations of internal/external pressure, torsion and axial load. It has been widely employed in investigations to study the failure behavior of tubular specimens under biaxial and triaxial loading [12].

Due to their microscopic heterogeneity, tubular specimens can fail in a variety of ways according to the structure of tubular specimen and the loading condition. The static and fatigue failure mechanisms of tubular specimens under multiaxial loading are almost researched experimentally through filament wound tubes and plain woven fabric tubes.

Kaddour A S [13] and Qi [14] studied the failure behavior of $\pm\theta$ filament wound tubes under various combinations of biaxial loads, matrix cracking was taken as the failure criterion. Fujii et al. [15-18] studied the static and fatigue failure behavior of plain woven fabric tubes under different combinations of tension-torsion loading, the failure mechanisms include delamination, matrix cracking and fiber breakage.

The aim of the present work is to examine the failure forms and failure strength of laminated tubes under different combinations of tension-torsion biaxial loading. Firstly, material properties of T700/epoxy are tested. Secondly, laminated tubes with $[45°/70°/-45°/0°_2]_s$ are tested under different combinations of tension-torsion biaxial loading. Thirdly, a progressive damage model is established to simulate the damage from initiation and propagation to the final catastrophic failure of tubular specimens, modified Hashin criteria are used to predict the strength of tubular specimens under different combinations of tension-torsion biaxial loading. Finally, some conclusions are drawn from the experimental and numerical studies.

Experimental investigation

Unidirectional (UD) T700/epoxy prepreg tape was used to manufacture all the unidirectional flat specimens and laminated tubular specimens.

Unidirectional flat specimens

According to ASTM D 3039-07 and ASTM D 3410-03, unidirectional flat specimens with off axis angles equal to 0°, 45° and 90° were prepared and tested on MTS 809 testing system. With the aid of strain rosettes, elasticity modulus and Poisson's ratio can be tested. Five specimens were tested for each material property. The results of elasticity modulus, Poisson's ratio and strength in each material principal direction are listed in Table 1.

Table 1. Material properties of T700/epoxy

	E_1	E_2	G_{12}	X_T	X_C	Y_T	Y_C	S_{12}	ν_{21}
	GPa	GPa	GPa	MPa	MPa	MPa	MPa	MPa	–
Average	106.5	6.77	3.23	1388.5	378.41	31.58	82.72	97.57	0.3476
Std. dev. (%)	5.26	4.06	5.46	5.09	5.05	2.24	9.78	7.19	9.33

Laminated tubular specimens

Some researchers [19, 20] tested laminated tubular specimens with different lay-ups under combined tension-torsion biaxial loading, such as $[90]_n$, $[0_F/90_{U,3}]$, $[0_F/90_{U,3}/0_F]$ and $[0/45/90/-45]_s$. For these lay-ups, there is a seam in the circumferential direction of all 90° plies in tubular specimen. The existence of the seam will lead to stress discontinuity. Theoretically and practically, 90° ply may never exist in laminated tubular specimens if no seam is required. Therefore, the stacking sequence of laminated tubular specimens is set as $[45°/70°/-45°/0°2]_s$ in this paper. The geometry of laminated tubular specimen is shown in Fig. 1.

All tubular specimens were tested on MTS 809 testing system for different combinations of tension-torsion biaxial loading. Four specimens were tested for each test condition.

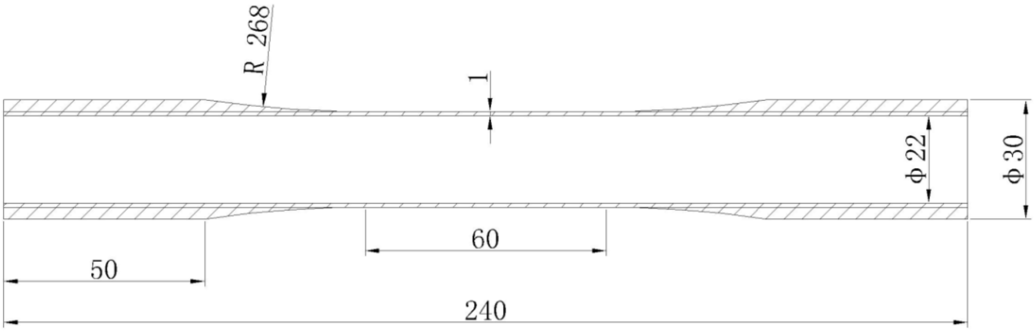

Figure 1. Geometry of tubular specimen (units in millimeters)

Experimental results

The final failure modes of tubular specimens under different combinations of tension-torsion biaxial loading are presented in Fig. 2. In appearance, the main fracture of every specimen lies in the middle of the gage section.

For every loading condition, matrix cracking is parallel to fibers, the fracture path of fiber is perpendicular to the direction of fiber in each layer, and delamination occurs around fiber breakage and matrix cracking. Even though all these kinds of failure modes occur in each biaxial loading condition, the damage degree of laminated tubes under different biaxiality ratio is different from each other, and the damage degree of laminated tubes becomes more and more serious along with the biaxiality ratio increases.

The biaxial strength of laminated tubes under different combinations of tension-torsion loading are listed in Table 2. It can be seen that as the biaxiality ratio decreases, the tensile strength decreases rapidly, while the torsional strength increases slowly. For instance, with A/T-2.2 as a standard, the tensile strength decreases by 64.46%, while the torsional strength only increases by 32.34% when biaxiality ratio equals to 0.6.

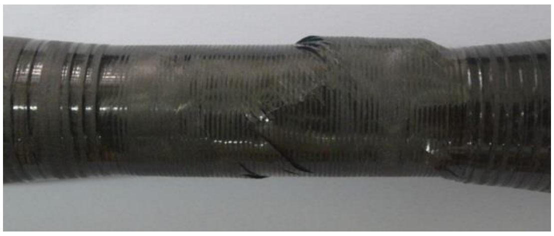

A/T-0

A/T-0.6

A/T-1.1

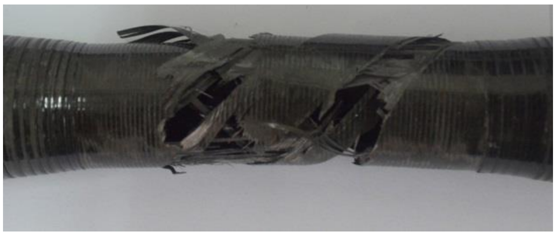

A/T-2.2

a. A/T is the biaxiality ratio (divide tension stress by torsion stress).

Figure 2. Failed tubular specimens under different combinations of tension-torsion loading

Table 2. Biaxial strength of laminated tubes under different different combinations of tension-torsion loading

Direction		A/T-2.2	A/T-1.1	A/T-0.6	A/T-0
Tensile strength	Experimental result (MPa)	332.48	190.79	118.18	-
	Std. dev. (%)	13.82	6.86	7.97	-
Torsional strength	Experimental result (MPa)	152.19	172.24	201.41	208.26
	Std. dev. (%)	15.39	9.27	5.12	7.76

Biaxial strength prediction model

Progressive damage model has been successfully utilized to study the failure behavior of composite materials under uniaxial static loading and uniaxial fatigue loading [21]. A typical progressive damage model comprises three major components: stress analysis, failure analysis and material property degradation rules. Progressive damage model can simulate the damage from initiation and propagation to the final catastrophic failure in detail. In this paper, the progressive damage model is extended for the failure analysis of laminated tubular specimens which is subjected to tension-torsion biaxial loading, and the flow chart is plotted in Fig. 3.

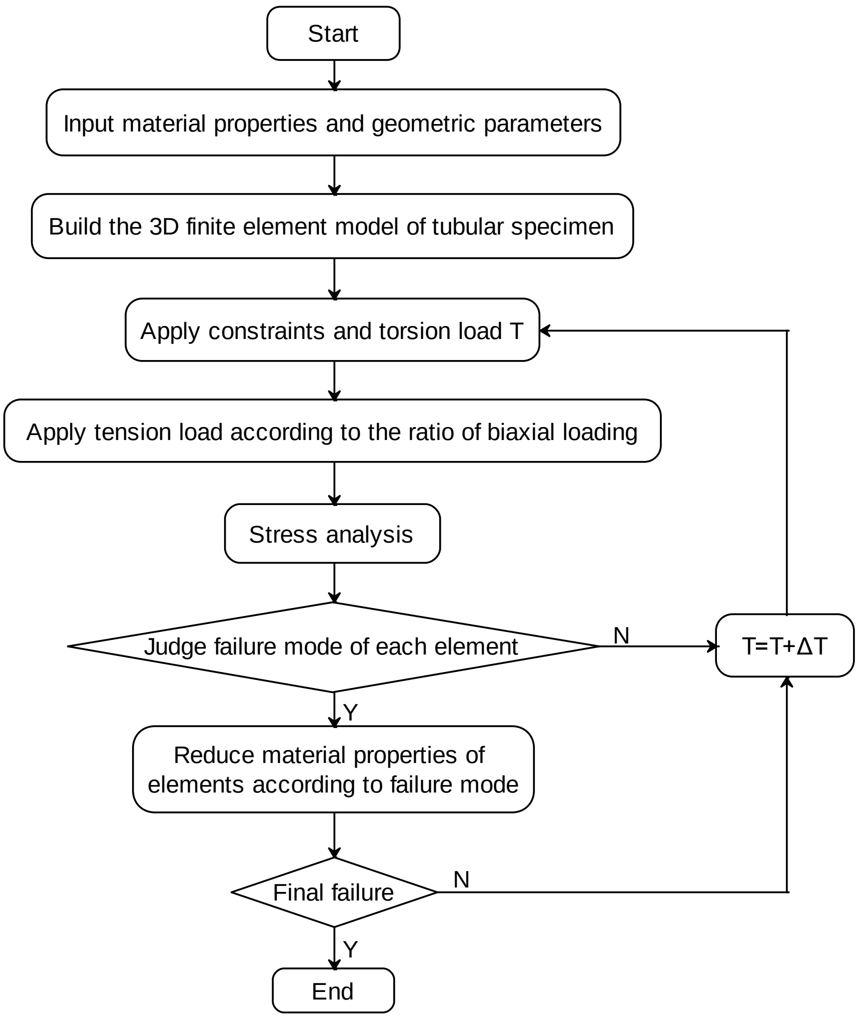

Figure 3. Flow chart of biaxial strength prediction model

Stress analysis

The first component of progressive damage model, the stress analysis, is explained in this section. For composite laminates or laminated tubular specimens without hole or any other cutouts, the stress field in the gauge section is homogeneous. However, the existence of end-tab in finite element model will cause significant stress concentrations near the end-tab. [22] According to failure criteria, these elements near the end-tab will be the first one to fail. This phenomenon is not consistent with experiment.

Based on above analysis, the tube was divided into three sections during the modeling process. As shown in Fig. 4, the middle one corresponds to the gauge section, and the other two sections correspond to the end-tab section. In the finite element model, all nodes on one end of the tube were all fixed, and all nodes on the other end of the tube were coupled with the node which lies on the axis of the tube. All tension and torsion loads were applied on this node which lies on the axis of the tube. During the progressive damage analysis, failure analysis and material property degradation were only applied on elements which belong to the gauge section. In this way, even though there are significant stress concentrations near the constraint region and the load region, the initial and final failure is caused by the homogeneous stress field in the gauge section.

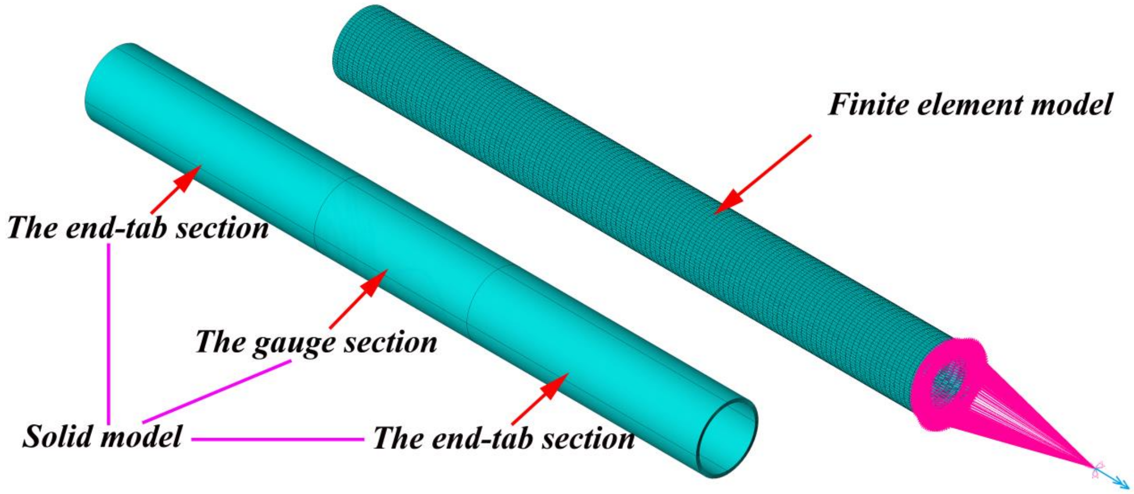

Figure 4. Solid model and finite element model of tubular specimen

Failure criteria

Due to their microscopic heterogeneity, composite materials present different failure modes under multiaxial state of stress. Fiber tensile/compressive failure, matrix tensile/compressive failure, tensile/compressive delamination failure and fiber-matrix shear failure are considered. Hashin [23] proposed a set of famous two-dimensional failure criteria for predicting the failure of composite materials. These criteria have been extensively applied in the progressive damage models. Modified three-dimensional Hashin failure criteria are used to predict the strength of tubular specimens under different combinations of tension-torsion biaxial loading. The specific expressions are given as follows:

(1) Fiber tensile failure ($\sigma_1 > 0$)

$$\left(\frac{\sigma_1}{X_T}\right)^2 + \left(\frac{\sigma_{12}}{S_{12}}\right)^2 + \left(\frac{\sigma_{13}}{S_{13}}\right)^2 - r^2 \geq 0 \tag{1}$$

(2) Fiber compressive failure ($\sigma_1 < 0$)

$$\left(\frac{\sigma_1}{X_C}\right)^2 - r^2 \geq 0 \tag{2}$$

(3) Matrix tensile failure ($\sigma_2 > 0$)

$$\left(\frac{\sigma_2}{Y_T}\right)^2 + \left(\frac{\sigma_{12}}{S_{12}}\right)^2 + \left(\frac{\sigma_{23}}{S_{23}}\right)^2 - r^2 \geq 0 \tag{3}$$

(4) Matrix compressive failure ($\sigma_2 < 0$)

$$\left(\frac{\sigma_2}{Y_C}\right)^2 + \left(\frac{\sigma_{12}}{S_{12}}\right)^2 + \left(\frac{\sigma_{23}}{S_{23}}\right)^2 - r^2 \geq 0 \tag{4}$$

(5) Tensile delaminaion failure ($\sigma_3 > 0$)

$$\left(\frac{\sigma_3}{Z_T}\right)^2 + \left(\frac{\sigma_{13}}{S_{13}}\right)^2 + \left(\frac{\sigma_{23}}{S_{23}}\right)^2 - r^2 \geq 0 \tag{5}$$

(6) Compressive delamination failure ($\sigma_3 < 0$)

$$\left(\frac{\sigma_3}{Z_C}\right)^2 + \left(\frac{\sigma_{13}}{S_{13}}\right)^2 + \left(\frac{\sigma_{23}}{S_{23}}\right)^2 - r^2 \geq 0 \tag{6}$$

(7) Fiber-matrix shear failure ($\sigma_1 < 0$)

$$\left(\frac{\sigma_1}{X_C}\right)^2 + \left(\frac{\sigma_{13}}{S_{13}}\right)^2 + \left(\frac{\sigma_{12}}{S_{12}}\right)^2 - r^2 \geq 0 \tag{7}$$

Where σ_i (i=1,2,3) are the normal stress components in each material principal direction, σ_{ij} (i, j=1,2,3) are the shear stress components, X_T, X_C, Y_T, Y_C, Z_T and Z_C represent tensile and compressive strength in longitudinal, transverse and normal direction, G_{ij} (i, j=1,2,3) and S_{ij} (i, j =1,2,3) represent the initial shear modulus and shear strength in ij plane, r is damage threshold.

Material property degradation rules

As failure occurs, material properties of failed elements are degraded. Some of the failure modes are catastrophic and some of them are not. A complete set of sudden material property degradation rules for all failure modes are given in Table 3.

Table 3. Material property degradation rules

Modes of failue	E_1	E_2	E_2	G_{12}	G_{13}	G_{23}	v_{12}	v_{13}	v_{23}
Fiber tensile failure	0.07	0.07	0.07	0.07	0.07	0.07	0.07	0.07	0.07
Fiber compressive failure	0.14	0.14	0.14	0.14	0.14	0.14	0.14	0.14	0.14
Matrix tensile failure	-	0.2	-	0.2	-	0.2	0.2	-	0.2
Matrix compressive failure	-	0.4	-	0.4	-	0.4	0.4	-	0.4
Tensile delaminaion failure	-	-	0	-	0	0	-	0	0
Compressive delamination failure	-	-	0	-	0	0	-	0	0
Fiber-matrix shear failure	-	-	-	0	0	-	0	-	-

Results and discussion

A summary of the biaxial strength of tubular specimens from experiments and the progressive damage model is presented in Fig. 5 and Table 4. The maximum error between predicted strength and experiments is within 9%.

Under tension-torsion biaxial loading, there will be shear stress in 0° plies, and the shear load carrying capacity of fiber is less than the axial load carrying capacity. Therefore, axial load carrying capacity of tubular specimen decreases rapidly as biaxiality ratio increases.

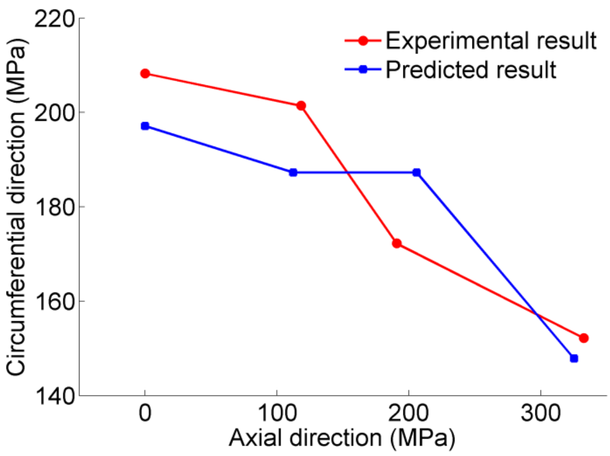

Figure 5. Biaxial strength of tubular specimens under tension-torsion loading

Table 4. Comparison of biaxial strength from the experiments and the model

Direction		A/T-2.2	A/T-1.1	A/T-0.6	A/T-0
Tensile strength	Experimental result (MPa)	332.48	190.79	118.18	-
	Predicted result (MPa)	325.26	206.00	112.36	-
	Error (%)	-2.17	7.97	-4.92	-
Torsional strength	Experimental result (MPa)	152.19	172.24	201.41	208.26
	Predicted result (MPa)	147.85	187.27	187.27	197.13
	Error (%)	-2.87	8.73	-8.51	-5.34

Conclusions

The present paper studied the biaxial strength of laminated tubes under tension-torsion biaxial loading experimentally and numerically. Firstly, the biaxial strength of laminated tubes with [45°/70°/-45°/0°2]s are tested under four different biaxial loading ratios. Secondly, a progressive damage model to simulate the failure behavior of laminated tubular specimens under different combinations of tension-torsion loading is proposed. The main advantage of the model is that it can simulate the failure behavior of laminated tubes under combined tension-torsion biaxial loading by using the experimental results of unidirectional flat specimens. The simulated tension/torsion strength show good agreement with experimental results. The experimental and numerical results show that the axial load carrying capacity decreases rapidly as the biaxiality ratio decreases. It should be noted that the progressive damage model proposed in this paper is a deterministic model, further research is needed to couple the defects for a more realistic simulation.

References

[1] Sun X S, Haris A, Tan V B C, et al., A multi-axial fatigue model for fiber-reinforced composite laminates based on Puck's criterion, *Journal of Composite Materials*, **46**, 2012, pp. 449-469.

[2] Busca D, Fazzini M, Lorrain B, et al., High-Speed Stereo Digital Image Correlation: Application to Biaxial Fatigue, *Strain*, **50**, 2014, pp. 417-427.

[3] Rheinfurth M, Schmidt F, Döring D, et al., Air-coupled guided waves combined with thermography for monitoring fatigue in biaxially loaded composite tubes, *Composites Science and Technology*, **71**, 2011, pp. 600-608.

[4] Smits A, Van Hemelrijck D, Philippidis T P, et al., Design of a cruciform specimen for biaxial testing of fibre reinforced composite laminates, *Composites Science and Technology*, **66**, 2006, pp. 964-975.

[5] Lecompte D, Smits A, Sol H, et al., Mixed numerical–experimental technique for orthotropic parameter identification using biaxial tensile tests on cruciform specimens, *International Journal of Solids and Structures*, **44**, 2007, pp. 1643-1656.

[6] Lamkanfi E, Van Paepegem W, Degrieck J, et al., Strain distribution in cruciform specimens subjected to biaxial loading conditions. Part 1: Two-dimensional versus three-dimensional finite element model, *Polymer Testing*, **29**, 2010, pp. 7-13.

[7] Lamkanfi E, Van Paepegem W, Degrieck J, et al., Strain distribution in cruciform specimens subjected to biaxial loading conditions. Part 2: Influence of geometrical discontinuities, *Polymer Testing*, **29**, 2010, pp. 132-138.

[8] Makris A, Vandenbergh T, Ramault C, et al., Shape optimisation of a biaxially loaded cruciform specimen, *Polymer Testing*, **29**, 2010, pp. 216-223.

[9] Serna Moreno M C, Curiel-Sosa J L, Navarro-Zafra J, et al., Crack propagation in a chopped glass-reinforced composite under biaxial testing by means of XFEM, *Composite Structures*, **119**, 2015, pp. 264-271.

[10] Serna Moreno M C, Martínez Vicente J L, López Cela J J, Failure strain and stress fields of a chopped glass-reinforced polyester under biaxial loading, *Composite Structures*, **103**, 2013, pp. 27-33.

[11] Smith E W, Pascoe K J, Biaxial fatigue of a glass-fibre reinforced composite,part 1: fatigue and fracture bahaviour, *Mechanical Engineering Publications*, 1989, pp. 367-396.

[12] Soden P D, Hinton M J, Kaddour A S, Biaxial test results for strength and deformation of a range of E-glass and carbon fibre reinforced composite laminates: failure exercise benchmark data, *Composites Science and Technology*, **62**, 2002, pp. 1489-1514.

[13] Kaddour A S, Soden P D, Hinton M J, Failure of ±55degree filament wound glassepoxy composite tubes under biaxial compression, *Journal of Composite Materials*, **32**, 1998, pp. 1618-1645.

[14] Dongtao Q, Guangxu C, Fatigue behavior of filament-wound glass fiber reinforced epoxy composite tubes under tension/torsion biaxial loading, *Polymer Composites*, **28**, 2007, pp. 116-123.

[15] Kawakami H, Fujii T J, Morita Y, Fatigue degradation and life prediction of glass fabric polymer composite under tension/torsion biaxial loadings, *Journal of Reinforced Plastics and Composites*, **15**, 1996, pp. 183-195.

[16] Fujii T, Lin F, Fatigue behavior of a plain-woven glass fabric laminate under tension/torsion biaxial loading, *Journal of Composite Materials*, **29**, 1995, pp. 573-590.

[17] Fujii T, Shiina T, Okubo K, Fatigue notch sensitivity of glass woven fabric composites having a circular hole under tension/torsion biaxial loading, *Journal of Composite Materials*, **28**, 1994, pp. 234-251.

[18] Fujii T, Amijima S, Lin F, Study on strength and nonlinear stress-strain response ofplain woven glass fiber laminates under biaxial loading, *Journal of Composite Materials*, **26**, 1992, pp. 2493-2510.

[19] Quaresimin M, Carraro P A, Damage initiation and evolution in glass/epoxy tubes subjected to combined tension-torsion fatigue loading, *International Journal of Fatigue*, **63**, 2014, pp. 25-35.

[20] Schmidt F, Rheinfurth M, Protz R, et al, Monitoring of multiaxial fatigue damage evolution in impacted composite tubes using non-destructive evaluation, *Composites Part A: Applied Science and Manufacturing*, **43**, 2012, pp. 537-546.

[21] Shokrieh M M, Lessard L B, Progressive fatigue damage modeling of composite materials, part I: Modeling, *Journal of Composite Materials*, **34**, 2000, pp. 1056-1080.

[22] Xiao Y, Kawai M, Hatta H, An integrated method for off-axis tension and compression testing of unidirectional composites, *Journal of Composite Materials*, **45**, 2011, pp. 657-669.

[23] Hashin Z, Failure Criteria for Unidirectional Fiber Composites, *Journal of Applied Mechanics*, **47**, 1980, pp. 329-334.